Combined Passive and Active Microwave Observations of Soil Moisture During CLASIC

Rajat Bindlish, *Senior Member, IEEE*, Thomas Jackson, *Fellow, IEEE*, Ruijing Sun, Michael Cosh, Simon Yueh, *Fellow, IEEE*, and Steve Dinardo

***Abstract*—An important research direction in advancing higher spatial resolution and better accuracy in soil moisture remote sensing is the integration of active and passive microwave observations. In an effort to address this objective, an airborne instrument, the passive/active L-band sensor (PALS), was flown over two watersheds as part of the cloud and land surface interaction campaign (CLASIC) conducted in Oklahoma in 2007. Eleven flights were conducted over each watershed during the field campaign. Extensive ground observations (soil moisture, soil temperature, and vegetation) were made concurrent with the PALS measurements. Extremely wet conditions were encountered. As expected from previous research, the radiometer-based retrievals were better than the radar retrievals. The standard error of estimates (SEEs) of the retrieved soil moisture using only the PALS radiometer data were 0.048 m^3/m^3 for Fort Cobb (FC) and 0.067 m^3/m^3 for the Little Washita (LW) watershed. These errors were higher than typically observed, which is likely the result of the unusually high soil moisture and standing water conditions. The radar-only-based retrieval SEEs were 0.092 m^3/m^3 for FC and 0.079 m^3/m^3 for LW. Radar retrievals in the FC domain were particularly poor due to the high vegetation water content of the agricultural fields. These results indicate the potential for estimating soil moisture for low-vegetation water content domains from radar observations using a simple vegetation model. Results also showed the compatibility between passive and active microwave observations and the potential for combining the two approaches.**

***Index Terms*—Active/passive microwave observations, hydrology, soil moisture, Soil Moisture Active Passive (SMAP).**

I. Introduction

MICROWAVE radiometry and radar are well-established techniques for soil moisture remote sensing. Currently, operating passive microwave satellite missions (Advanced Microwave Scanning Radiometer and WindSat) that provide soil moisture products have limited spatial resolution (25–40 km). On the other hand, current spaceborne radars provide very high spatial resolution (10 m) observations. However, progress in developing robust soil moisture retrieval algorithms using microwave radar observations has been limited. This is, in part, associated with the influence of a wide range of other variables on the radar response. The revisit time for a specific high-resolution radar system is very long. For example, the Advanced Land Observing System (ALOS) phased array L-band synthetic aperture radar has a return period of 45 days, which limits the type of soil moisture algorithms that can be used, such as temporal change.

A National Aeronautics and Space Administration (NASA) satellite currently under development, the Soil Moisture Active Passive (SMAP) mission, will soon address these limitations. SMAP will collect both active and passive L-band data. It will focus on using higher resolution radar in conjunction with the radiometer to produce a high accuracy and improved spatial resolution product with high temporal frequency. Other less optimal but still important opportunities using L-band include the European Space Agency Soil Moisture Ocean Salinity mission combined with the Japanese Aerospace Exploration Agency ALOS radar and the NASA Aquarius instrument with low-resolution passive and active microwave.

At the core of the SMAP mission concept is the idea that combining the information from passive (surface emissivity) and active (backscatter signatures) sensors can improve the accuracy and spatial resolution of the mission's geophysical parameter retrieval. Although there have been numerous sets of either passive or active microwave data collected in conjunction with soil moisture observations, there have been very few that included both [1], [2]. In order to explore these new algorithm concepts, an experiment was conducted that would collect prototype SMAP data. This experiment was embedded in the cloud and land surface interaction campaign (CLASIC) that was conducted over the Southern Great Plains in June 2007. As part of CLASIC, passive/active L-band sensor (PALS) data were collected over a one-month period to support the combined algorithm concept.

II. Field Experiment Description

To investigate the benefits of combining passive and active microwave sensors, the Jet Propulsion Laboratory developed an airborne PALS for measurements of soil moisture and ocean salinity [2]. The PALS has a dual-polarization radiometer and polarimetric radar. For CLASIC, PALS was flown on a Twin Otter aircraft over the Little Washita (LW) and Fort Cobb (FC) watersheds in Oklahoma. A total of 11 days were flown over a one-month period in June/July 2007. The instrument was flown at an altitude of 1100 m above ground level, which resulted in an instantaneous footprint size of approximately 400 m.

The topography of the region is moderately rolling with a maximum relief less than 200 m. Soils include a wide range of textures with large regions of both coarse and fine textures.

Manuscript received September 15, 2008; revised January 22, 2009. Current version published October 14, 2009. The work described in this letter was supported by the National Aeronautics and Space Administration.

R. Bindlish is with Science Systems and Applications Inc., Hydrology and Remote Sensing Laboratory, Agricultural Research Service, U.S. Department of Agriculture, Beltsville, MD 20705 USA.

T. Jackson, R. Sun, and M. Cosh are with the Hydrology and Remote Sensing Laboratory, Agricultural Research Service, U.S. Department of Agriculture, Beltsville, MD 20705 USA.

S. Yueh and S. Dinardo are with the Jet Propulsion Laboratory, Pasadena, CA 91109 USA.

Digital Object Identifier 10.1109/LGRS.2009.2028441

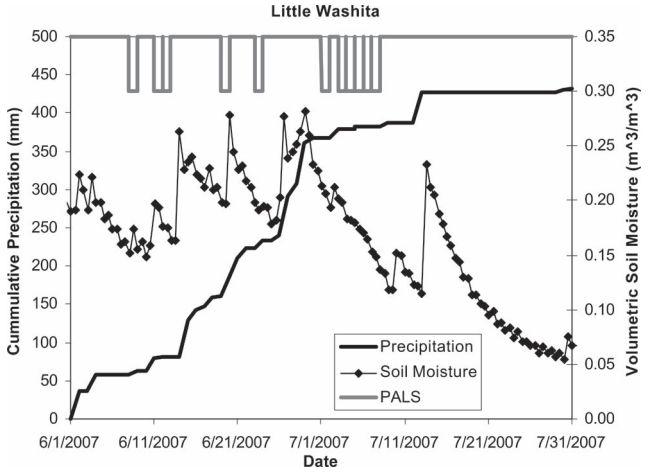

Fig. 1. Cumulative average precipitation and soil moisture observations (from *in situ* sensors) over the LW watershed during CLASIC. The 11 days of PALS flights over the watershed are also shown.

The region in Oklahoma is exceptionally well instrumented for surface soil moisture, hydrology, and meteorology research. Both the LW and FC watersheds have a dense network of *in situ* soil moisture and rain gauge sites.

The aircraft flights were designed to include a set of lines over intensively sampled fields. Fields were located close together and with general locations that minimized the number of flightlines. During the experiment, 27 fields (15 in LW and 12 in FC) of size $\sim$800 m $\times$ 800 m were sampled for soil moisture and related variables.

Extreme rainfall conditions were encountered during the CLASIC field experiment. The summer precipitation over the Southern Great Plains in 2007 was significantly greater than the average and resulted in new historic records in many areas. This rainfall resulted in widespread and repeated flooding throughout Oklahoma and Texas and, consequently, in very wet conditions throughout the duration of the experiment (Fig. 1). Persistent cloud cover, saturated soil (that slowed infiltration), and senescent winter wheat fields, which could not be harvested, reduced evapotranspiration that would typically occur from the soil surface. All factors contributed to water-logged winter wheat fields.

LW received about 400 mm of precipitation during June 2007, and observed soil moisture at the sampling locations was between 0.20 and 0.40 $\mathrm{m}^3/\mathrm{m}^3$ during the experiment. As a result, the soil moisture retrieval algorithms could only be validated for moderate to very wet conditions.

III. PALS Mapping

PALS is a fixed single-beam radiometer with an incidence angle of 40°. The current version of PALS does not have an imaging capability. In order to construct images during CLASIC, the PALS was flown on ten adjacent east–west flightlines. The distance between two flightlines was 800 m. PALS observations over LW were gridded and mapped at a 400-m resolution.

Fig. 2 shows the gridded H-polarization PALS brightness temperatures. The brightness temperatures on the eastern and western parts of the watershed are lower than in the middle. The central part of the watershed is predominantly sandy soils, whereas the eastern and western parts are mostly loam. The sandier soils drain quicker and typically have lower soil moisture due to their smaller field capacity. The central part is mostly rangeland, whereas the eastern and western parts are mostly winter wheat and agricultural crops. The brightness temperature pattern observed was consistent to L-band observations made during previous LW experiments [3], [4].

Fig. 3 shows the gridded HH-polarization PALS backscatter coefficient. The eastern and western parts of the watershed have lower backscatter coefficients. As noted earlier, radar responses from land surfaces depend upon many factors that include soil moisture, vegetation, and roughness. Vegetation and surface roughness have a first-order effect on the radar observations. The backscatter coefficient typically increases with an increase in soil moisture. Surface roughness and vegetation both have an opposite effect on the backscatter coefficient as compared with soil moisture. An increase in surface roughness or vegetation leads to increase in scattering, which results in lower backscatter coefficient measurements (more negative). In the eastern and western portions of the watershed, we observed lower backscatter coefficients even though they had higher soil moisture. These areas have winter wheat or agricultural crops with higher amounts of vegetation that can result in greater scattering. The spatial patterns of the backscattering images were consistent throughout the duration of the experiment.

IV. PALS Soil Moisture Results

A. Radiometer-Based Retrievals

PALS footprint observations within each sampling site were averaged to obtain a field average. The field-average brightness temperature observations were then used in a soil moisture retrieval algorithm [5]. *In situ* soil moisture and soil temperature measurements were made at each sampling site concurrent with the PALS observations. Vegetation water content measurements were also made during the experiment. Based upon field observations of general conditions during CLASIC, the vegetation parameters and water content for the senescent winter wheat and pasture fields were assumed to be constant over the period. Vegetation parameters and water content for the agricultural fields were linearly interpolated as a function of time.

Fig. 4 shows the comparison between the observed and the PALS radiometer-based soil moisture estimates for the LW and FC watersheds. The dynamic range of soil moisture for the intensive sampling sites was 0.20–0.45 $\mathrm{m}^3/\mathrm{m}^3$ on the days with PALS coverage. The PALS estimated soil moisture compared well with the *in situ* observations. The soil moisture estimates for FC $(\mathrm{SEE} = 0.048\ \mathrm{m}^3/\mathrm{m}^3)$ were better than for the LW watershed $(\mathrm{SEE} = 0.067\ \mathrm{m}^3/\mathrm{m}^3)$. This may be due to the smaller size of the FC mapping domain as well as differences in land cover types and soils. Some error is likely to be associated with the occurrence of standing water, which could not be accounted for in the soil moisture retrieval.

B. Radar-Based Retrievals

Vegetation canopies complicate the retrieval of moisture in the underlying soil because the canopies also contain water. Due to scattering effects, the interaction between the two contributions is highly nonlinear. In order to account for these problems, a simple approach, based on the water-cloud model,

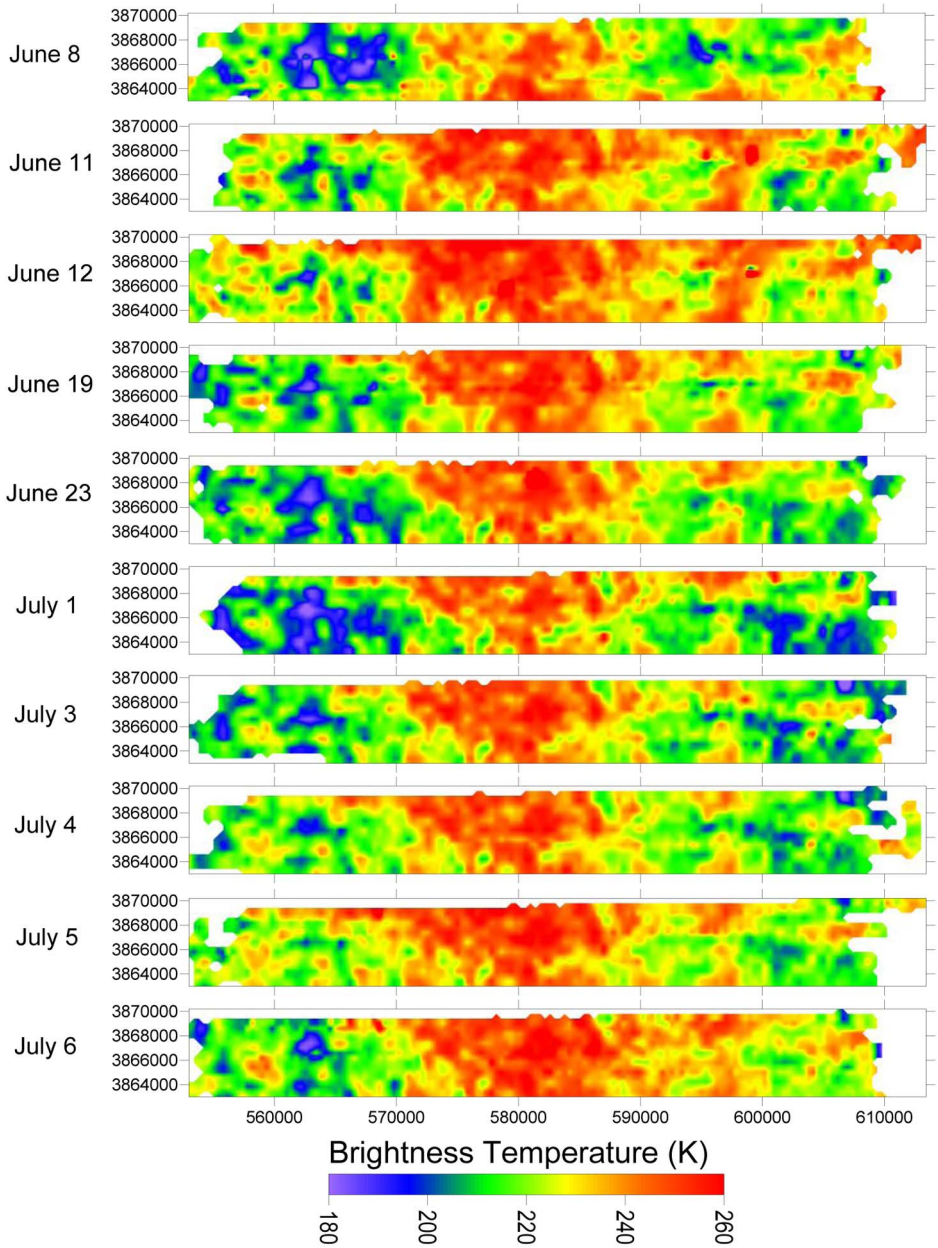

Fig. 2. PALS L-band H brightness temperature observations over the LW watershed. The brightness temperatures were mapped in Universal Transverse Mercator (UTM) coordinates (zone 14).

was developed by Attema and Ulaby [6]. They represented the canopy in a radiative transfer model as a uniform cloud whose spherical droplets are held in place structurally by dry matter. In water-cloud models, the canopy is represented by "bulk" variables such as leaf-area index or total water content. Because of the parsimonious use of parameters, these models can be easily inverted. Therefore, this approach is a good candidate for use as the basis of a retrieval algorithm. Basic conceptual assumptions in the water-cloud model include the following: 1) the vegetation is represented as a homogeneous horizontal cloud of identical water spheres, uniformly distributed throughout the space defined by the soil surface and the vegetation height; 2) multiple scattering between canopy and soil can be neglected; and 3) the only significant variables are the height of the canopy layer and the cloud density, the latter assumed to be proportional to the volumetric water content of the canopy. Bindlish and Barros [7] used this approach to retrieve soil moisture from Spaceborne Imaging Radar C-band (SIR-C) observations over the LW watershed.

For a given incidence angle θ, the backscatter coefficient is represented in water-cloud models by the general form

$$\sigma^o = \sigma^o_{\text{veg}} + \sigma^o_{\text{veg+soil}} + \tau^2 \sigma^o_{\text{soil}} \tag{1}$$

where τ^2 is the two-way vegetation transmissivity. The first term represents the scattering due to the vegetation canopy, the second term represents the interaction between the vegetation canopy and the soil underneath and accounts for multiple scattering effects, and the third term represents the scattering from the soil layer. The vegetation–soil interactions are neglected in

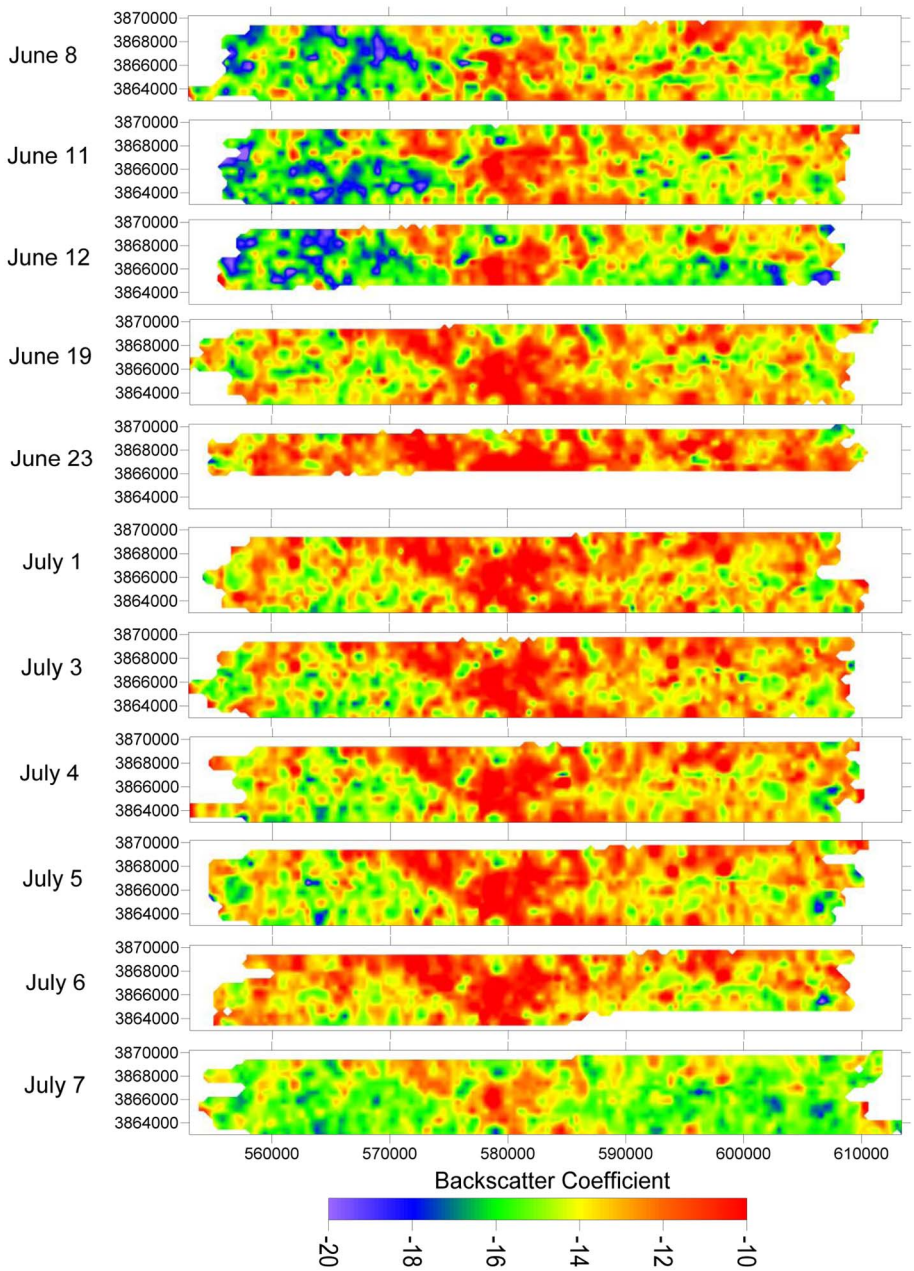

Fig. 3. PALS L-band HH backscatter coefficient observations over the LW watershed. The backscatter coefficients were mapped in UTM coordinates (zone 14).

the water-cloud model, and the vegetation term for HH and VV is given by [8]

$$\sigma^o_{\text{veg}} = 0.74\alpha\left(1 + 0.54\alpha\tau - 0.24(\alpha\tau)^2\right) \times [1 - \exp(-2.12\tau\sec\theta)]\cos\theta \quad (2)$$

where α is the single-scattering albedo. This formulation corresponds to the first-order solution of the radiative transfer equation through a weak medium, where multiple-scattering effects can be neglected. This term becomes significant as the vegetation canopy increases. The vegetation–soil interaction models typically are more complicated and require additional information. Despite its simplicity, the water-cloud model has been shown to provide fair-to-good agreement with experimental data [7], [9].

Here, PALS observations at HH and VV were used to estimate soil moisture. The vegetation backscattering effect was computed using the water-cloud model. The vegetation parameters were assumed to be the same for both HH and VV polarizations. The soil-surface backscattering coefficient was computed using the Dubois model [10]. This model was developed using SIR-C data collected over the LW watershed and is valid for bare soil and low vegetation conditions. Soil moisture observations from June 11 and July 3 were used to estimate the roughness coefficient for each sampling site. These roughness coefficients were then used to compute the soil moisture for all the flight days.

Fig. 5 shows the comparison between the *in situ* observed and estimated soil moisture for the LW and FC watersheds. The radar retrievals for the LW ($\text{SEE} = 0.079\ \text{m}^3/\text{m}^3$) are

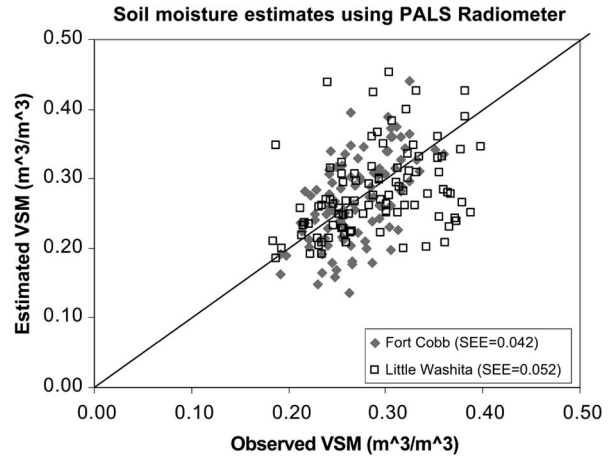

Fig. 4. Comparison between *in situ* soil moisture observations and PALS radiometer-based estimates for the LW and FC watershed mapping domains.

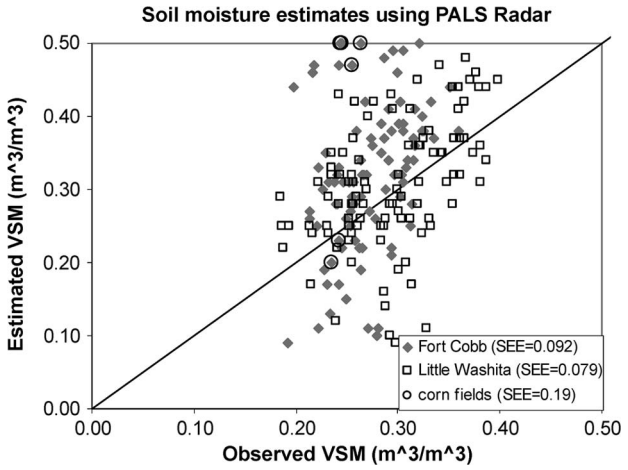

Fig. 5. Comparison between *in situ* soil moisture observations and PALS radar-based estimates for the LW and FC watershed mapping domains.

better than those for FC $(\mathrm{SEE} = 0.092\ \mathrm{m}^3/\mathrm{m}^3)$. The estimates are particularly poor for fields with higher vegetation (corn) $(\mathrm{SEE} = 0.19\ \mathrm{m}^3/\mathrm{m}^3)$. The model estimated very high soil moisture over the corn field during the second half of the experiment when the vegetation water content was high $(\mathrm{VWC} > 4\ \mathrm{kg}/\mathrm{m}^2)$. The use of a simplified approach has its caveats and limitations. As the vegetation canopy increases, the error associated with the vegetation–soil interaction increases, leading to poor soil moisture estimates. Increase in vegetation canopy increases the observed radar backscatter. Ignoring this term leads to overestimation of soil moisture for areas with high vegetation. This is one of the reasons for the poor soil moisture estimates for corn canopies (Fig. 5). Over the FC domain, the estimated soil moisture exhibits a higher dynamic range than the observations. The estimated soil moisture has a low bias for both the domains. The presence of high vegetation results in higher soil moisture estimates.

V. Discussion and Summary

Results showed that the PALS brightness temperature and backscatter observations were consistent with observed ground conditions. In addition, the brightness temperature pattern observed over LW was consistent with previous investigations. The radiometer-based soil moisture retrieval captured the observed dynamic range and showed no significant bias for both watersheds. Considering the extreme wet conditions, the estimated soil moisture compared reasonably well with the *in situ* observations.

One of the shortcomings in soil moisture remote sensing is the lack of a robust radar algorithm. Most of the radar algorithms have been developed and tested over limited areas. These algorithms need to be validated over multiple domains in order to develop a global radar soil moisture algorithm. Here, a model-based approach was developed and applied with success. Further testing of this modeling approach should be conducted over multiple domains, which could lead to a robust radar algorithm for bare soil and moderate vegetation domains.

As mentioned earlier, extremely wet conditions were encountered during the experiment. These wet conditions resulted in saturated soils and standing water in many fields. These conditions were likely to be present in parts of the PALS footprints. Further analyses of the CLASIC data sets should attempt to quantify the effect of standing water on brightness temperature and backscatter observations, which may lead to reduction in errors.

The validation of the CLASIC PALS data sets presented here establishes a baseline performance for conventional methods of soil moisture retrieval using either a radiometer or radar. Further research will focus on developing integrated radar–radiometer soil moisture algorithms using PALS radiometer and radar observations.

References

[1] E. Njoku, W. Wilson, S. Yueh, S. Dinardo, F. Li, T. Jackson, V. Lakshmi, and J. Bolten, "Observations of soil moisture using a passive and active low frequency microwave airborne sensor during SGP99," *IEEE Trans. Geosci. Remote Sens.*, vol. 40, no. 12, pp. 2659–2673, Dec. 2002.

[2] U. Narayan, V. Lakshmi, and E. Njoku, "Retrieval of soil moisture from passive and active L/S band sensor (PALS) observations during the Soil Moisture Experiment in 2002 (SMEX02)," *Remote Sens. Environ.*, vol. 92, no. 4, pp. 483–496, Sep. 2004.

[3] T. J. Jackson, D. M. Le Vine, C. T. Swift, T. J. Schmugge, and F. R. Schiebe, "Large area mapping of soil moisture using the ESTAR passive microwave radiometer in Washita'92," *Remote Sens. Environ.*, vol. 54, no. 1, pp. 27–37, Oct. 1995.

[4] T. J. Jackson, D. M. Le Vine, A. Y. Hsu, A. Oldak, P. Starks, C. T. Swift, J. Isham, and M. Haken, "Soil moisture mapping at regional scales using microwave radiometry: The Southern Great Plains hydrology experiment," *IEEE Trans. Geosci. Remote Sens.*, vol. 37, no. 5, pp. 2136–2151, Sep. 1999.

[5] T. J. Jackson, "Measuring surface soil moisture using passive microwave remote sensing," *Hydrol. Process.*, vol. 7, no. 2, pp. 139–152, 1993.

[6] E. P. W. Attema and F. T. Ulaby, "Vegetation modeled as a water cloud," *Radio Sci.*, vol. 13, no. 2, pp. 357–364, 1978.

[7] R. Bindlish and A. P. Barros, "Parameterization of vegetation backscatter in radar-based soil moisture estimation," *Remote Sens. Environ.*, vol. 76, no. 1, pp. 130–137, Apr. 2001.

[8] H. J. Eom and A. K. Fung, "A scatter model for vegetation up to Ku-band," *Remote Sens. Environ.*, vol. 15, no. 3, pp. 185–200, Jun. 1984.

[9] T. Mo, T. J. Schmugge, and T. J. Jackson, "Calculation of radar backscattering coefficient of vegetation cover soils," *Remote Sens. Environ.*, vol. 15, no. 2, pp. 119–133, Mar. 1984.

[10] P. C. Dubois, J. Van Zyl, and E. T. Engman, "Measuring soil moisture with imaging radars," *IEEE Trans. Geosci. Remote Sens.*, vol. 33, no. 4, pp. 915–926, Jul. 1995.